Configuration Effects on Acoustic Performance of a Duct Liner

Carl H. Gerhold [1], Martha C. Brown[2], Michael G. Jones[3], Douglas Nark[4]
NASA Langley Research Center, Hampton, Virginia

Brian M. Howerton[5]
Lockheed-Martin Mission Services, Hampton, Virginia

Abstract

Continued success in aircraft engine noise reduction necessitates ever more complete understanding of the effect that flow path geometry has on sound propagation in the engine. The Curved Duct Test Rig (CDTR) has been developed at NASA Langley Research Center to investigate sound propagation through a duct of comparable size (approximately ½ the gap of GE90) and physical characteristics to the aft bypass duct of typical aircraft engines. The liner test section is designed to mimic the outer/inner walls of an engine exhaust bypass duct that has been unrolled circumferentially. Experiments to investigate the effect of curvature along the flow path on the acoustic performance of a test liner are performed in the CDTR and reported in this paper. Flow paths investigated include both straight and curved with offsets from the inlet to the discharge plane of ½ and 1 duct width, respectively. The test liners are installed on the side walls of the liner test section. The liner samples are perforate over honeycomb core, which design is typical of liners installed in aircraft nacelles. In addition to fully treated side walls, combinations of treated and acoustically rigid walls are investigated. While curvature in the hard wall duct is found not to reduce the incident sound significantly, it does cause mode scattering. It is found that asymmetry of liner treatment causes scattering of the incident mode into less attenuated modes, which degrades the overall liner attenuation. It is also found that symmetry of liner treatment enhances liner performance by eliminating scattering into less attenuated modes. Comparisons of measured liner attenuation with numerical results predicted by an analytic model based on the parabolic approximation (CDUCT-LaRC) have also been made and are reported in this paper. The effect of curvature in the rigid wall configuration estimated by CDUCT-LaRC is similar to the observed results, and the mode scattering seen in the measurements also occurs in the analytic model results. The analytic model and experiment show similar differences of overall attenuation between one wall treated and both walls treated.

[1] Senior Research Engineer, Aeroacoustics Branch, phone: (757) 864-5279, email: carl.h.gerhold@nasa.gov, Associate Fellow, AIAA
[2] Aerospace Engineer, Aeroacoustics Branch, phone: (757) 864-6277, email: martha.c.brown@nasa.gov
[3] Senior Research Scientist, Structural Acoustics Branch, phone: (757) 864-5272, email: michael.g.jones@nasa.gov, Associate Fellow, AIAA
[4] Aerospace Engineer, Structural Acoustics Branch, phone: (757) 864-5784, email: d.m.nark@nasa.gov, Member, AIAA
[5] Staff Engineer, Langley Program Office, phone: (757) 864-8365, email: brian.m.howerton@nasa.gov, Member, AIAA

I. Introduction

Acoustically absorbing liners are a proven means to reduce turbofan tone noise in aircraft engines. Single degree of freedom liners, in the form of a honeycomb core sandwiched between a perforate cover sheet and impervious backing sheet, are the most common implementations in the fan inlet and aft bypass duct, where a significant component of the noise is tonal[1]. The honeycomb core structure implies an acoustic impedance boundary condition (acoustically locally reacting) that has provided enormous computational savings for the implementation of duct propagation models in practical design applications. This acoustic predictability, along with their light weight and physical robustness, has made these structures the design choice for over four decades. Although propagation model prediction accuracy has generally been adequate, new engine duct configurations, with reduced area available for liners, is likely to place renewed emphasis on the need for greater prediction accuracy. Methods have been developed to determine the impedance of a single degree of freedom liner sample based on acoustic measurements, and are used extensively by researchers at NASA Langley Research Center [2,3]. Minner and Rice developed a computer code to estimate the far field noise radiation from the inlet and exhaust of a turbofan engine, which includes the effects of liners[4]. A multi-year program combined the efforts of NASA, industry, and academia to investigate methods to analyze and predict the performance of established liner technologies, and to investigate new concepts[5]. Jones, et al[6] reported on an extensive study to evaluate and catalog the effect of design parameters such as per cent open area of the perforate and ratio of perforate thickness to hole diameter on the acoustic performance of single degree of freedom, perforate over honeycomb liners. Mean flow in the duct is known to increase the resistance of the liner face sheet and to shift the reactance curve to higher frequencies[7].

While the performance of liners in a laboratory setting is well identified, the installation effect can affect liner performance significantly. Specifically, the geometry of the duct is an installation parameter of interest. Cummings[8] investigated analytically and experimentally the propagation of sound through a hard wall square duct with 180° turn. He found that the transmission coefficient through the curve was unity throughout the frequency range studied, indicating that all the incident energy was transmitted through the hard wall bend. However, the sound pressure profile varied across the duct, and the variation increased as the radius of curvature increased relative to the wavelength of the sound. This study was limited to frequencies for which only (0,0) mode was cut on. Furnell and Bies[9] solved for reflection and transmission of sound as it propagated through an elliptical hard wall duct with a curve. They found that curve tended to alter the radial mode structure into a form that had the appearance of a higher order mode. Fuller and Bies[10] reported a theoretical and experimental investigation of the sound propagation through a 180° hard wall bend with a centrally located splitter. They found significant insertion loss at discrete frequencies over the range up to cut on of the (1,0) mode. The splitter added significantly to the impedance mismatch seen by the incoming plane wave at particular frequencies. While these investigations are limited to plane wave propagation in 180° turns, they suggest that the hard wall curved duct does alter the mode composition of the incoming wave.

Changes in the duct configuration other than bends can have an effect on sound propagation. Boija and Nillson[11] performed an analytical study of the effect of sudden area discontinuities and sharp edges on scattering of incident sound. McAlpine and Wright[12] reported on analytical investigation of the effect of splices on sound propagation in a lined duct. They investigated scattering of incident energy into higher order azimuthal modes, and noted that the scattered energy effect was greater at lower engine speeds.

The present paper is a report on the investigation of configuration effects, such as curvature of the flow path and non-symmetry of the duct liner treatment in a full size duct and in the presence of higher order modes. The experimental program makes use of the Curved Duct Test Rig (CDTR). In a previous paper, Gerhold, et al[13], discuss the development of the CDTR as a research tool whose purpose it is to improve the understanding of the behavior of duct treatment in ducts such as the aft bypass duct. The bypass duct flow path is often curved to accommodate the engine core, and the CDTR is designed to address the effect of curvature on sound propagation, with the aim of determining whether curvature can be used to enhance liner performance. The test section cross-section is rectangular in order to simplify the design and manufacture of candidate duct liner configurations. The experimental rig is relatively large, the test section dimensions scale to approximately 50% of the bypass duct gap of a GE90. This allows for modes of order higher than (0,0) to propagate. The mode content of the sound can be controlled so that a user-specified mode is incident on the liner test section.

A second purpose of the CDTR is to provide a test bed with which to validate analytical models of sound propagation in the duct. The experimental results reported in this paper are compared to results from computer code, CDUCT-LaRC, which is based on the parabolic approximation to the convected Helmholtz equation.

II. Description of the Experiment

Figure 1 is a photograph of the Curved Duct Test Rig. A brief description of the test rig will be presented here, and more complete description of the rig can be found in previous papers by the authors[13,14]. Air is supplied to the test rig from a centralized air supply and passes through a set of mufflers (not shown in the photograph), an elbow with turning vanes, and a flow conditioning section to smooth the air flow and reduce turbulence. A transition section reduces the duct cross section from 0.76 m x 0.76 m (30 inch x 30 inch) to the test section, which is 0.15 m x 0.38 m (6 inch x 15 inch). Downstream of the test section is a diffuser, which reduces the air flow speed and provides an anechoic termination. The test section consists of 6 duct sections: the source, two measurement, two filler, and the liner test section. The source section contains an array of 16 loudspeakers arranged around the duct. The loudspeaker positions are chosen to maximize the transfer of acoustic energy into the duct in all cut on modes. There are two measurement sections with microphones, one upstream of the liner test section and one downstream. The microphone arrays are identical in both sections, containing 47 flush-mounted B&K model 4951, 6.4 mm (1/4-inch) piezoceramic microphones. Selection of

the microphone locations to maximize resolution of the modal decomposition is discussed in reference 13. A subarray consisting of 31 of the microphones in upstream array is used to measure the error signal for the control system that generates the sound in the duct. The purpose of the control system is to isolate a targeted mode in the duct at a user-specified amplitude at the inlet to the liner test section. The liner test section contains the sample of liner under investigation. The top and bottom walls of the liner test section are 12.7 mm (1/2 -inch) thick aluminum plate and the liner samples form the side walls. Figure 2 shows the straight flow path liner sample in place on both side walls of the liner test section. This liner sample is 38.1 cm (15 inch) high and 81.3 cm (32 inch) long in the flow direction. The space behind the liner sample is filled with a stiff and rigid foam block that is used to hold the liner samples in place. Through bolts affix the liner sample firmly against the rigid foam and the wall of the liner test section. The straight and curved liner samples were fabricated by Goodrich Aerostructures, and hard wall versions were fabricated in-house using the same design. Finally, two 20.3 cm (8 inch) long rigid wall duct sections are on either end of the liner test section. Their purpose is to separate the microphones from the near field effects due to sudden impedance discontinuities at either end of the liner.

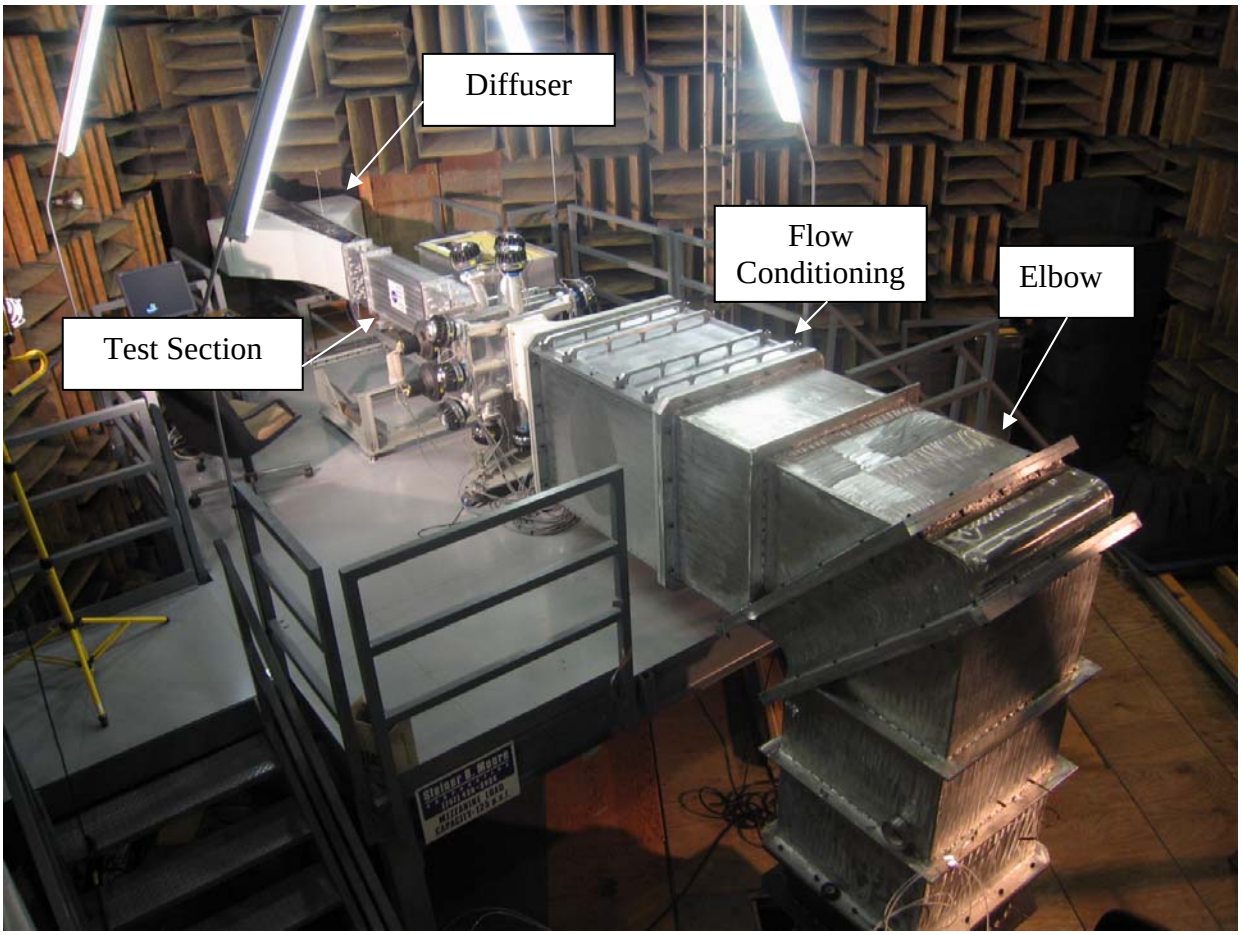

Figure 1. Curved Duct Test Rig in the Anechoic Noise Research Facility.

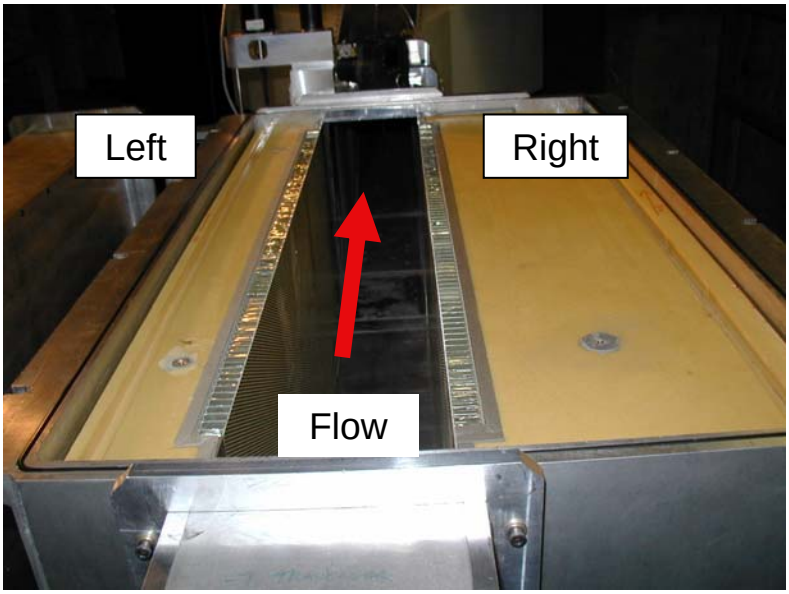

Figure 2. Liner test section with straight Goodrich liner on both walls, top removed, view looking downstream

The liners consist of an impervious backing sheet, 19.1 mm (0.75-inch) thick honeycomb core, and perforate cover sheet. The perforate sheet thickness is 0.64 mm (0.025 inch). The perforate is 8.7% open area with 0.99 mm (0.039-inch) diameter holes. The liner design parameters are chosen to be representative of single degree of freedom liners in use in engines. The resonance frequency of the liner installed in the CDTR occurs in the middle of the operating range of the CDTR, between 300 and 2400 Hz.

In addition to the straight path, two curved path configurations were fabricated. The outlet flange in the first configuration is offset from the inlet by ½ duct dimension (7.62 cm) and in the second configuration the offset is 1 duct dimension (15.24 cm). The liner test section with the 1D offset liner sample installed is shown in Figure 3.

The curves of the liners are designed so that the slope increases linearly from zero at the inlet to a maximum at the mid point and then decreases linearly from the midpoint to the discharge, where the slope is zero. The radius of curvature is 17.4 cm (44.2 inch) for the 1D offset and 33.9 cm (86.1 inch) for the ½ D offset. Hard wall equivalents of the liner samples were fabricated using the same design parameters but in which the perforate cover sheet was replaced with a solid sheet.

Various configurations of hard and treated wall were evaluated and are summarized in Table I. The liner samples are identified by the configuration designation Cabcd, where 'a' is 1 for straight flow path, 2 for ½ duct dimension offset, and 3 is for 1 duct dimension offset; 'b' is S for soft wall or H for hard wall on the left side of the duct (looking downstream); 'c' is S for soft wall or H for hard wall on the right side of the duct (looking downstream); and 'd' is N for no flow or F for flow on at Mach 0.275. Thus configuration C1SHN is straight path, soft wall on the left and hard wall on the right, flow off. Note

that no data were acquired for two conditions; straight flow path, soft wall on the left and hard wall on the right, flow on at Mach 0.275 and for curved, ½ D offset, soft wall both sides, flow on at Mach 0.275.

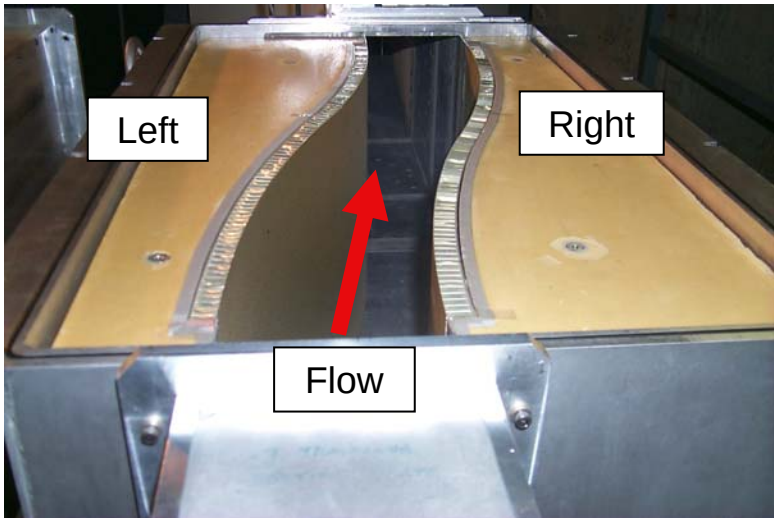

Figure 3. 1 D offset curved liner sample in the liner test section of the CDTR (top removed), view looking downstream.

Flow Path	Liner Description	Flow	
		M=0.000	M=0.275
Straight	Both wall treated	C1SSN	C1SSF
Straight	Right wall treated, left wall hard	C1HSN	C1HSF
Straight	Left wall treated, right wall hard	C1SHN	X
Straight	Both wall hard	C1HHN	C1HHF
½-D offset	Both wall treated	C2SSN	X
1-D offset	Both wall treated	C3SSN	C3SSF
1-D offset	Right wall treated, left wall hard	C3HSN	C3HSF
1-D offset	Left wall treated, right wall hard	C3SHN	C3SHF
1-D offset	Both wall hard	C3HHN	C3HHF

Table I. Liner sample testing configurations, X indicates no data acquired

Tonal acoustic excitation, over the frequency range 300 to 2400 Hz, is generated upstream of the liner test section. The sound is controlled such that a user-specified mode shape propagates in the duct. Vertical mode orders ranging from 0 to 5, and horizontal mode orders from 0 to 2 can be isolated by the control system. The controlled mode is generally at least 10 dB higher than any other cut on mode in the duct. The system is capable of operating with flow, the maximum condition of which is uniform flow outside the boundary layer through the liner test section at Mach 0.275. Table II shows the frequencies at which the horizontal (n) and vertical (m) modes are expected to cut on in the duct at standard conditions. Horizontal modes in the CDTR correspond to radial modes in the engine bypass duct and vertical modes in the CDTR correspond to circumferential modes. The cut on frequencies for no flow are the first set of numbers and

the cut on frequencies when uniform flow is present in the duct at Mach 0.275 are shown in parentheses.

n (horiz) / m (vert)	0	1	2
0	0	1128 (1084)	2256 (2168)
1	451 (434)	1215 (1168)	2301 (2211)
2	902 (867)	1445 (1388)	2430 (2335)
3	1354 (1301)	1762 (1693)	
4	1805 (1734)	2128 (2045)	
5	2256 (2168)		

Table II. Cut-on frequencies of modes in the 15.2 cm (horizontal) x 38.1 cm (vertical) duct at standard conditions. Values without parentheses are at Mach 0.0, values within parentheses are with flow at Mach 0.275

III. Analysis Methodology

The expressions for the liner attenuation and the modal power ratio are given in this section. The acoustic power is derived in the rigid wall duct with uniform flow in which the sound source is a pure tone at frequency ω. This formulation is used because, in the experiment, the sound is measured in rigid wall sections upstream and downstream of the liner. The experimentally determined attenuation is the ratio of the acoustic power upstream to the acoustic power downstream expressed in dB. In addition to the liner attenuation, this determination includes the effects of reflections at the leading and trailing edges of the liner and reflections from the duct termination. Sound reflection from the leading edge of the liner is generally observed to be small. The duct termination has been designed to minimize sound reflection[13]. The calculated attenuation based on experimental data is compared to predicted attenuation using the CDUCT-LaRC computation.

A. Attenuation Computation from Measured Data

The CDTR control system, which is described in greater detail in reference 13, adjusts the amplitude and phase of each of the acoustic driver outputs in order to isolate a tone at the target mode shape and amplitude. Once the convergence criteria for mode amplitude are met, the data acquisition commences. Sound is measured, first from the 47 microphones in the upstream array with channel 48 recording a reference signal from the control system, then from 47 microphones (and the reference signal) in the array downstream of the liner test section. The data for each array are collected at a rate of 25,600 samples/second for 20 seconds. Five hundred (500) non-overlapping, 1024-point Digital Fourier Transforms are performed, using the reference to lock the phase of each microphone signal relative to a common phase, and the average spectrum is computed. The complex-value voltage spectra are converted to complex sound pressure in pascals using magnitude and phase calibration factors. The complex pressures in the bin corresponding to the excitation frequency are formed into a vector of length 94 (47 for

the upstream and downstream arrays). These complex-valued pressure vectors are processed in a modal decomposition routine to determine the complex-valued modal amplitudes for the waves in the duct, both positive-traveling (incident) and negative-traveling (reflected). The analysis includes all the cut-on modes and the two lowest cut-off modes above the excitation frequency. In a previous paper[13] the authors outlined the procedure by which sound measured at the duct walls is used to determine the complex amplitudes of the modes. The modal amplitudes are used to determine the sound pressure and acoustic velocity of each modal component in a method outlined in a previous paper by the authors[14]. The sound pressure p_{mn} and acoustic velocity u_{mn} are used to evaluate Morfey's[15] expression for the axial acoustic intensity of the (m,n) modal component, I_{mn}, in uniform axial flow:

$$I_{mn}(x,y,z) = \frac{1}{2}\left\{ \Re\left[(1+M_o^2)\, p_{mn} u_{mn}^*\right] + M_o\left[\frac{p_{mn} p_{mn}^*}{\rho_o c_o} + \rho_o c_o u_{mn} u_{mn}^* \right] \right\} \tag{1}$$

where:
ρ_o = air density (kg/m^3)
c_o = speed of sound (m/sec)
M_o = Mach number
* signifies complex conjugate
$\Re$ = real part of the complex quantity

The sound power ϕ_{mn} of the (m,n) component of the wave is evaluated by integrating the intensity over the cross section of the duct:

$$\phi_{mn}(z) = \int_0^b \int_0^a I_{mn}(x,y,z)\, dx\, dy \tag{2}$$

The attenuation of the liner is determined from the log of the ratio of sound power upstream of the liner to the power downstream, summed over all modes:

$$\Delta dB = 10 \log_{10}\left[\frac{\sum_n \sum_m \phi_{mn}(z_u)}{\sum_n \sum_m \phi_{mn}(z_d)} \right] \tag{3}$$

Another parameter, in addition to the overall attenuation, is employed to characterize the scatter of incident acoustic energy. The redistribution of modal energy is determined by evaluating the sound power in the (m,n) mode in the downstream hard wall section, normalized by the total sound power in the upstream section:

$$\text{Power Ratio} = \left[\frac{\phi_{mn}(z_d)}{\sum_n \sum_m \phi_{mn}(z_u)} \right] \tag{4}$$

Note that, since the sound upstream is dominated by the incident component of the target mode, the total power upstream is predominantly the power of the incident component of the target mode.

B. Computations from CDUCT-LaRC

The CDUCT-LaRC[16] duct propagation and acoustic radiation tool was developed to study the internal acoustic propagation within and radiation from complex three dimensional duct geometries. The code is composed of five distinct modules: input and output specification, Computational Fluid Dynamics and acoustic grid generation, background flow calculation, duct acoustic propagation and acoustic radiation. The propagation module, which was used in this study, currently incorporates the work of Dougherty[17, 18] and utilizes a parabolic approximation to the convected Helmholtz equation. This approach affords very efficient propagation calculations, thus allowing solutions for complex three-dimensional geometries to be handled with relatively low computational costs. This efficiency comes at the expense of reduced accuracy when modes close to cut-off are considered or when the flow path is highly curved. In these cases, the direction of propagation of the particular duct mode diverges from the preferred angle of the parabolic approximation, which is parallel to the duct axis. Additionally, loss of accuracy may occur when reflection of acoustic waves in the axial direction becomes important, as reflected waves are not captured in this formulation. These two limitations of the parabolic approximation may lead to differences between measured and computed attenuations.

In modeling the CDTR, a three block structured grid as shown in figure 4 is used for the CDUCT-LaRC predictions. In this figure, acoustic propagation is taken to be from left to right. The block boundaries are set such that upstream (left-most) block is fully hardwall and begins at the termination of the upstream microphone array. The interior block captures the treated portion of the CDTR with treatment locations shown as shaded green and white wireframe surfaces in figure 4. Finally, the downstream (right-most) block is fully hardwall and extends from the treatment termination to the axial location of the first microphone in the downstream microphone array. The multi-block approach allows a treatment specification scheme that is independent of grid spacing. The acoustic source, specified at the first axial plane of the upstream block, is comprised of hardwall rectangular mode amplitudes and relative phases obtained from the upstream microphone set. Modal decomposition is performed at the last axial plane of the downstream block.

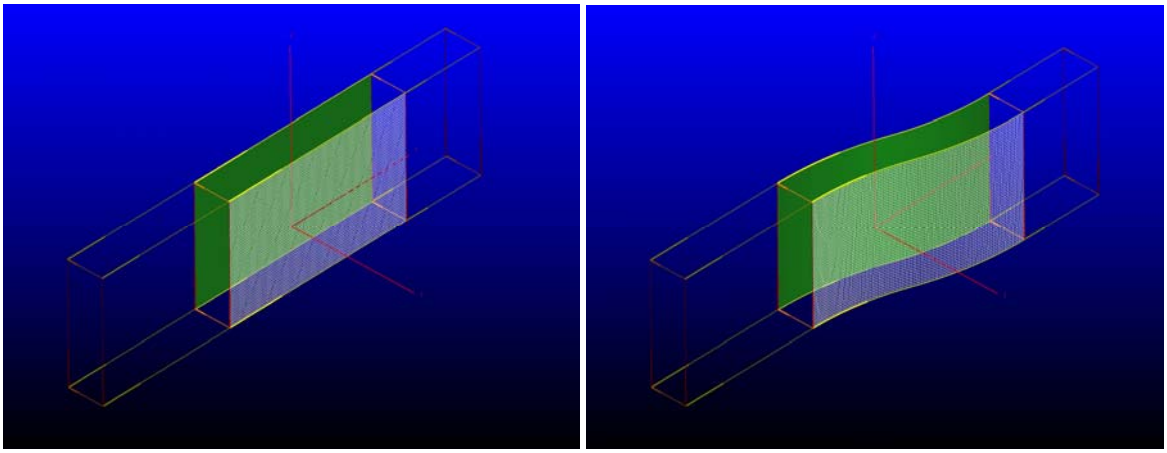

(a) Straight Configuration (b) 1 D Offset Configuration

Figure 4: CDTR Prediction Domain

IV. Results

In the sections to follow, figures that illustrate a significant point are included in the body of the paper. Figures that demonstrate a trend for higher order modes are collected in Appendix A.

As indicated previously, data were collected with air flow off and with air flow on at Mach 0.275. The results for no flow only are included in this paper.

A. Effect of curvature-Hard wall duct.

Hard wall samples of the straight and the 1D offset curved liners were fabricated and evaluated in the liner test section of the Curved Duct Test Rig. These tests are intended to demonstrate the effect of duct curvature on sound propagation. Because the duct is hard wall, albeit curved, no attenuation of the input wave is expected. This is found to be nearly the case as is shown in Figure 5. The figure shows the attenuation in the liner test section for the hard wall liner samples with a (0,0) mode wave incident on the liner test section, and compares the straight hard wall configuration (C1HHN) to the 1 D offset curved hard wall configuration (C3HHN). Most of the incident energy is conserved through the liner test section. The average power loss across all frequencies is 1.2 dB in the straight section, and is 1.2 dB for the curved section. The walls are not perfectly rigid and the wall compliance is responsible for approximately 1 dB of energy loss. The wall curvature accounts for less than 0.5 dB attenuation.

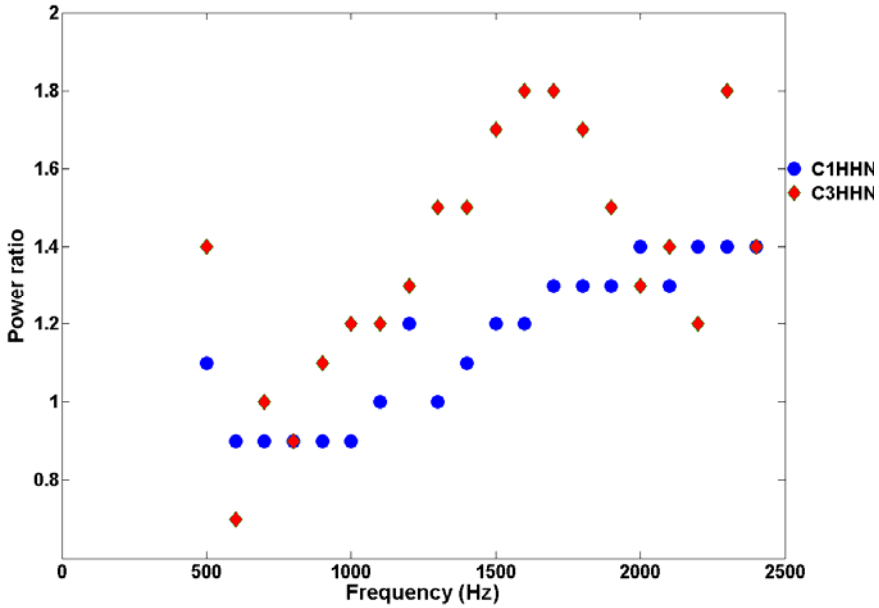

Figure 5. Attenuation in hard wall liner test section for 0,0 mode wave incident, no flow, compares straight section (C1HHN) to curved at 1D offset (C3HHN).

The downstream modal energy distribution for the (0,0) mode incident on the liner test section with straight hard wall sample is shown in Figure 6. It is seen that the (0,0) mode is clearly dominant downstream of the liner test section. When the (0,0) mode is incident on the curved liner test section, the mode is reduced significantly beginning at approximately 800 Hz, as can be seen on Figure 7. Energy is transferred into the next higher horizontal mode, the (0,1) mode, once it cuts on at 1200 Hz. The energy loss between 800 and 1200 Hz is felt to be due to absorption by the compliant fabricated hard wall. The higher vertical orders of the horizontal order 0 mode similarly transfer energy into the horizontal order 1 mode when they are incident upon the curved hard wall liner. This is seen in Figure A-1 for the (1,0) mode, Figure A-2 for the (2,0) mode, and Figure A-3 for the (3,0) mode.

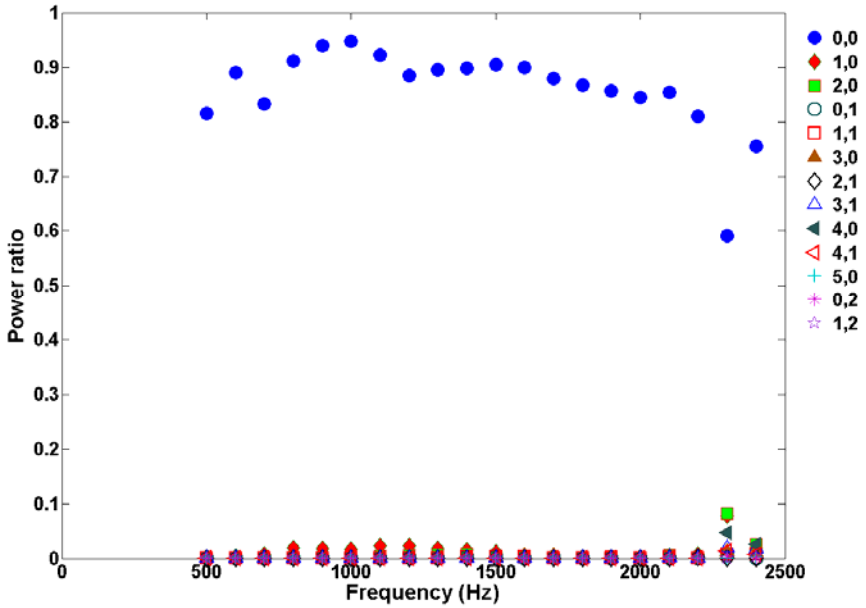

Figure 6. Modal energy distribution downstream of liner test section with straight hard wall sample (C1HHN), (0,0) mode wave incident, no flow.

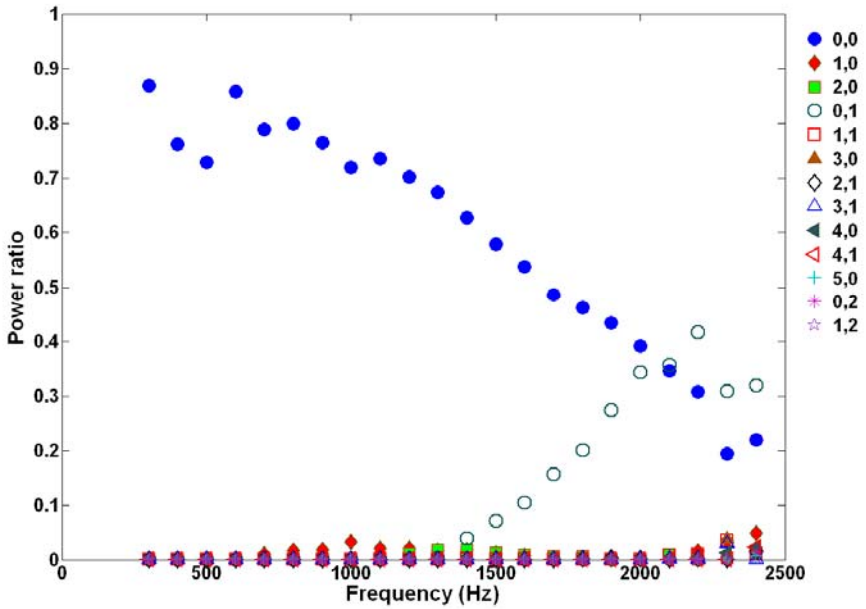

Figure 7. Modal energy distribution downstream of liner test section with curved hard wall sample (C3HHN), (0,0)mode wave incident, no flow.

Figure 8 shows the modal energy distribution for the (0,1) mode incident upon the liner test section with 1D offset curved hard wall sample. In this case, the energy transfers, not to the next higher horizontal mode, but to the next lower, (0,0) mode. In a similar manner, higher vertical orders of the horizontal order 1 mode scatter into the horizontal

order 0 mode. This is illustrated in Figure A-4, where the (1,1) incident mode scatters energy into the (1,0) mode.

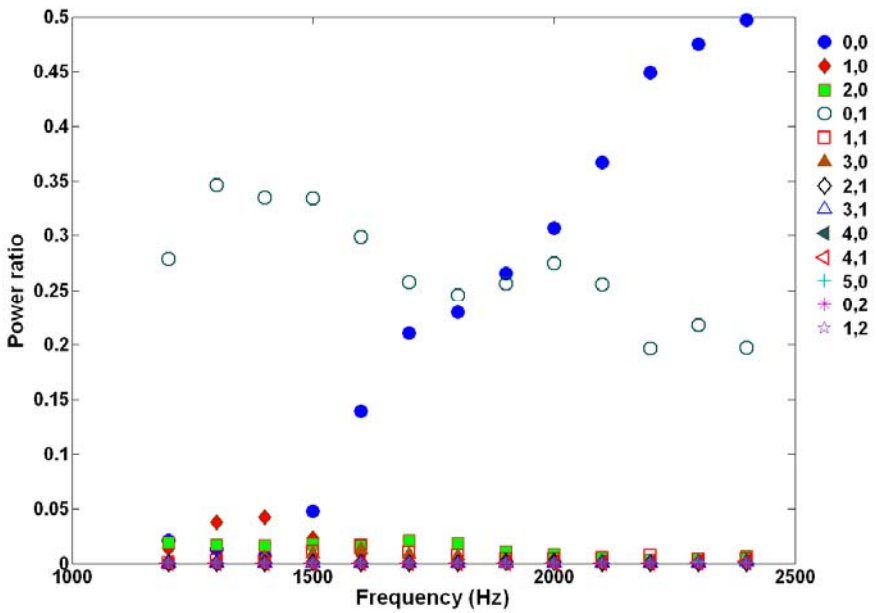

Figure 8. Modal energy distribution downstream of liner test section with curved hard wall sample (C3HHN), (0,1) mode wave incident, no flow.

B-1. Effect of curvature- one wall treated-overall attenuation

A series of experiments was performed in which one wall of the liner test section was hard walled and the other was treated with the perforate over honeycomb liner. This was done for both the straight liner test section and the 1D offset curved section. Configurations included treated wall on the left side with the right side hard wall and treated wall on the right side with the left side hard wall. The right side treated case is presented here since there was little discernible difference between the two cases.

The overall attenuation with (0,0) mode wave incident on the liner test section with one wall treated is shown in Figure 9. The straight C1HHN and curved C3HHN cases are compared in the figure. The peak attenuation occurs at 1600 Hz and, except near the peak and at high frequencies, there is very little difference between the results for the straight and curved liners. The attenuation at the peak is greater for the curved liner section than for the straight, but the attenuation curve tapers off less quickly above the peak for the straight liner than it does for the curved liner. Similar results are seen in Figure A-5 for the (1,0) mode incident.

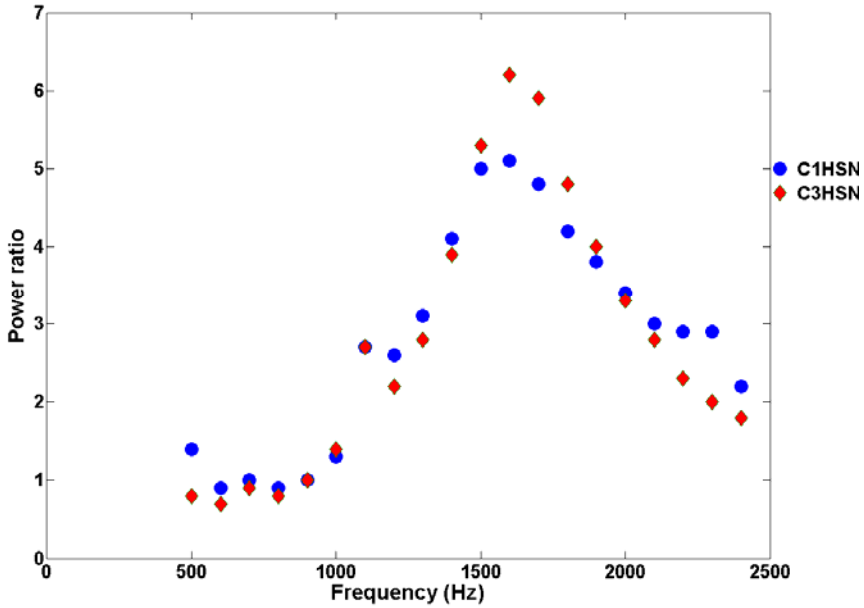

Figure 9. Attenuation of (0,0) mode wave incident on liner test section with right side acoustically treated, left side hard wall. Compares straight liner sample (C1HSN) with 1D offset curved sample (C3HSN)

When horizontal order 1 modes are incident on the liner test section, the peak of the attenuation curve shifts upward to between 2100 and 2200 Hz, see Figure10 for the (0,1) mode and Figures A-6 and A-7 for the (1,1) and (2,1) modes, respectively. The straight and curved liner attenuation curves are quite similar up to approximately 1900 Hz. At higher frequencies the straight liner consistently provides greater attenuation than the curved liner.

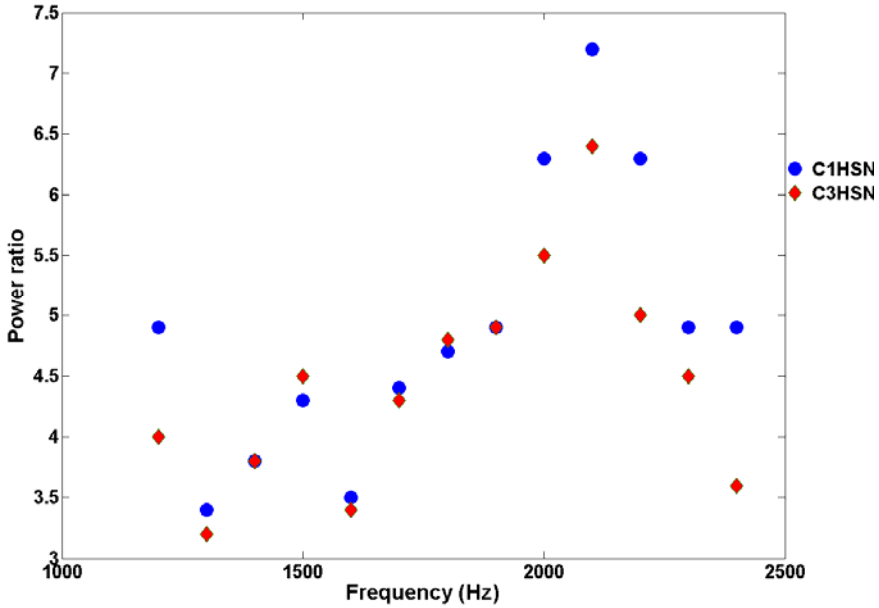

Figure 10. Attenuation of (0,1) mode wave incident on liner test section with right side acoustically treated, left side hard wall. Compares straight liner sample (C1HSN) with 1D offset curved sample (C3HSN)

B-2. Effect of curvature- one wall treated-distribution of modes

Figure 11 shows the modal distribution of the power ratio for the 1D offset curved liner C3HSN with (0,0) mode wave incident on the liner test section. The (0,0) mode is decreased significantly. The figure shows that incident energy in the (0,0) mode component is transferred to the (0,1) mode. The (0,1) mode is less attenuated at the frequency of peak attenuation of the incident mode, so that the overall sound at the attenuation peak is dominated by the (0,1), resulting in an overall attenuation of 6 dB, as was observed in Figure 9. The transfer of energy from the incident horizontal order 0 mode into the less attenuated horizontal order 1 mode is also seen in the energy distribution for (1,0) incident case, Figure A-8. Figure 12, the energy distribution for the (3,0) mode incident on the curved liner, shows an interesting feature. The (3,1) mode cuts on at a frequency above the frequency of peak attenuation and thus does not contribute to the total energy. Thus, for the (3,0) mode incident, the scattered energy does not affect the overall attenuation appreciably.

The energy in modes of horizontal order 1 scatters into horizontal order 0 modes that are less attenuated. This is shown in Figure 13, where energy incident on the liner test section is predominantly in the (1,1) mode, but the energy downstream is as strong in the (1,0) mode as in the (1,1).

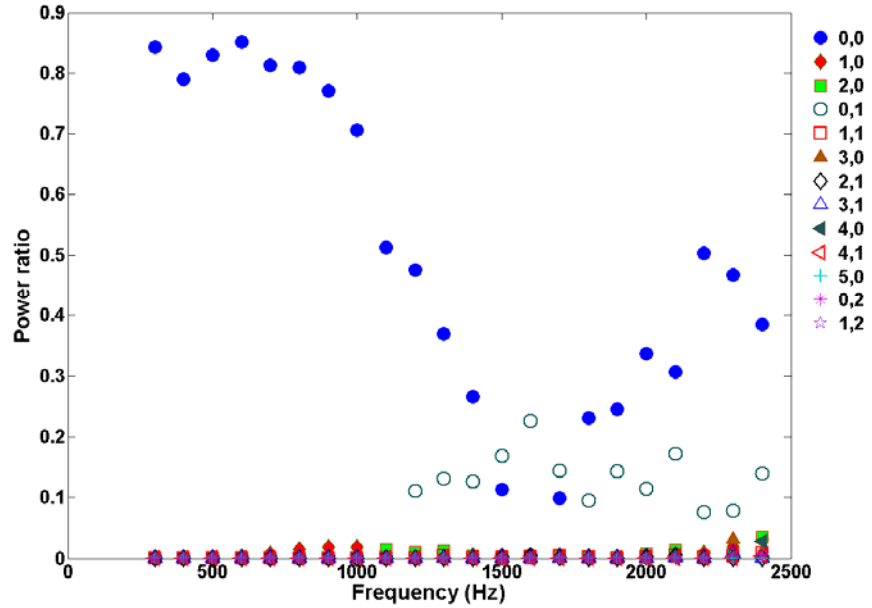

Figure 11. Modal energy distribution downstream of liner test section with 1D offset curved test section lined on one side (C3HSN), (0,0) mode wave incident, no flow.

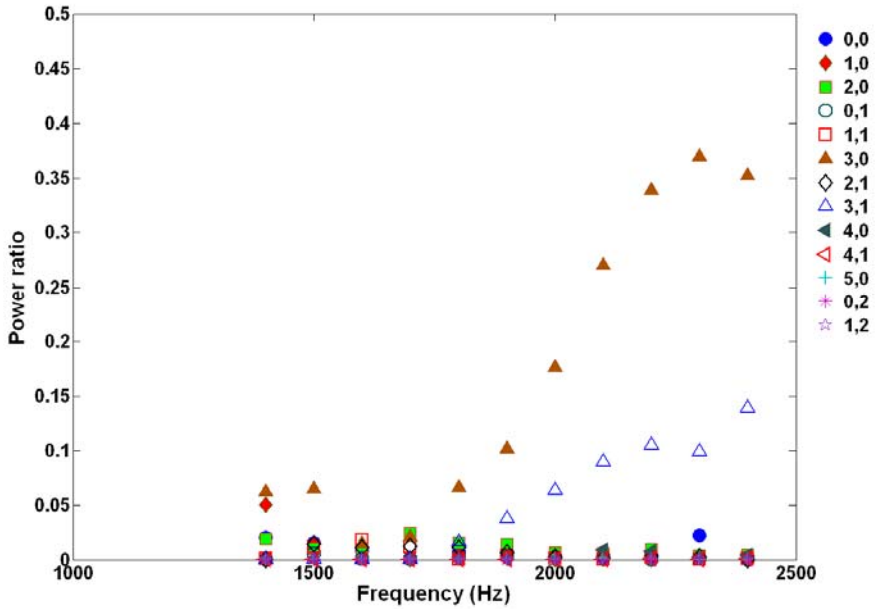

Figure 12. Modal energy distribution downstream of liner test section with 1D offset curved test section lined on one side (C3HSN), (3,0) mode wave incident, no flow.

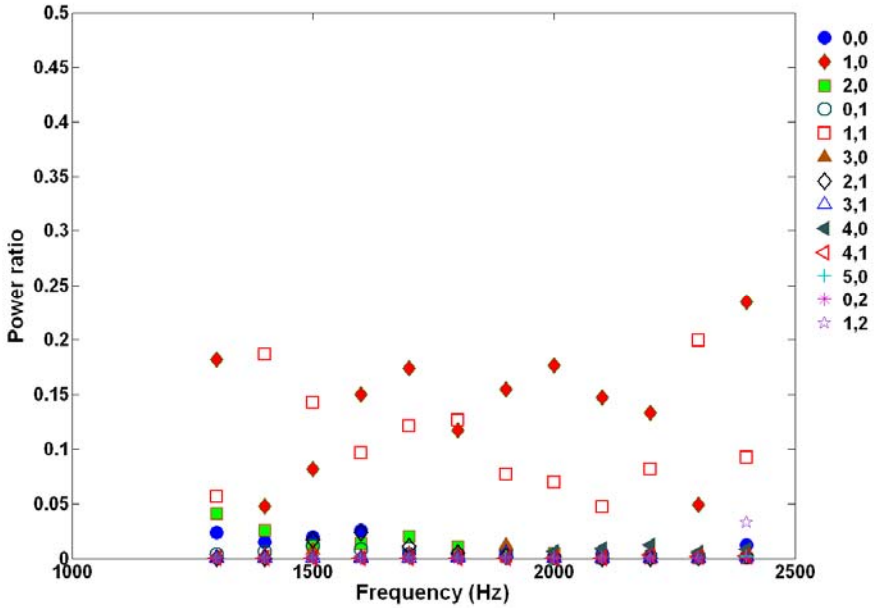

Figure 13. Modal energy distribution downstream of liner test section with 1D offset curved test section lined on one side (C3HSN), (1,1) mode wave incident, no flow.

C. Both walls treated

The attenuation for both walls of the liner test section acoustically treated is shown in Figure 14 for (0,0) mode incident on the liner test section. The results are shown for overall attenuation for the straight liner, the ½ D offset, and 1 D offset liner configurations. The peak attenuation occurs at 1800 Hz, and it ranges from 22 dB for the 1D offset to 29 dB for the straight liner.

It is expected that doubling the liner area would double the attenuation. However, comparing Figure 14 to Figure 9 shows that the maximum overall attenuation for both sides lined is more than double the attenuation of the one wall lined configuration. The overall attenuation in the single wall lined configuration was reduced by mode scattering into a less attenuated mode. When both walls are lined, no appreciable energy is transferred into less attenuated modes as can be seen in Figure 15 for the straight configuration.

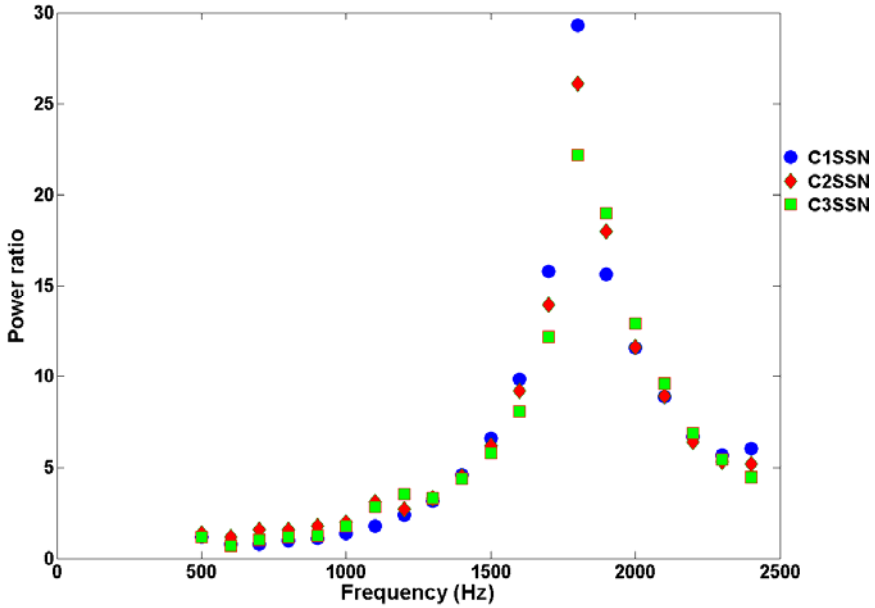

Figure 14. Attenuation of incident (0,0) mode wave, liner treatment on both sides, compares straight liner (C1SSN), 1/2D offset curved (C2SSN), and 1D offset curved (C3SSN)

Figure 14 also shows that the attenuation curves are quite similar for the straight (C1SSN), ½ D offset (C2SSN), and 1D offset (C3SSN) liner samples, except near the peak. Interestingly the maximum attenuation is greatest for the straight liner sample and the maximum attenuation decreases as the offset increases. This trend is seen for higher order modes as well. Two possible explanations for the variation in the attenuation with curvature are being explored, the effect of resonator skew and the effect of incidence angle. Parrott et al[19] investigated the effect of skewing the resonator channel incidence angle away from normal in an effort to lengthen the resonator cavity without increasing overall liner depth. They found that when the cavity was skewed without changing cavity depth, the first resonance and anti-resonance frequencies remained the same, but the resistance changed, increasing with increasing skew angle. The authors did not discuss the effect of the resistance change on attenuation by the liner, but it is expected that changing the resistance will change the attenuation, particularly at the peak. The depth of the honeycomb liner is held constant in fabrication of the curved liner samples in the current study and the cavity is effectively skewed from normal. Thus the resonant frequency of the liner should not change with curvature, but the resistance could. Since the resistance dominates liner performance at resonance, any change of resistance would be seen most clearly at the peak of the attenuation curve. The angles of skew in the study by Parrott et al were 30° and 60°, respectively. The maximum angle of the curved liners is 21° for the 1D offset liner. Thus it may be that further analysis will show that the skew angle is not sufficient to explain the observed change of attenuation. Another possible explanation is the change of angle of incidence of the wave due to liner curvature. Motsinger and Kraft[20] show the dependence of the liner absorption, not only on the resistance and reactance of the liner, but also on the angle of incidence. The absorption is

strongly dependent on incidence angle at the resonance condition where the reactance is close to 0. Further research is underway in the current experiment to quantify the effect that curvature has on duct liner performance.

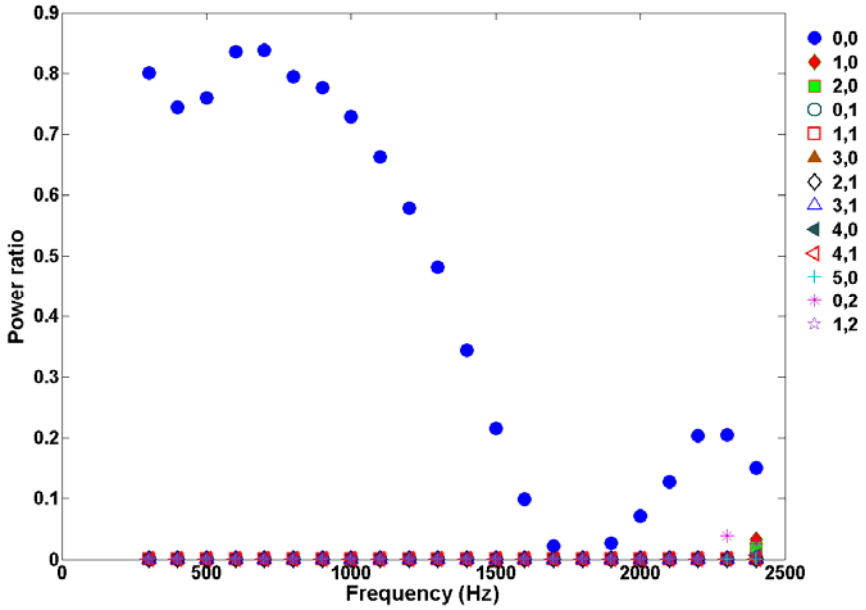

Figure 15. Modal energy distribution downstream of liner test section with straight test section lined on both sides (C1SSN), (0,0) mode wave incident, no flow.

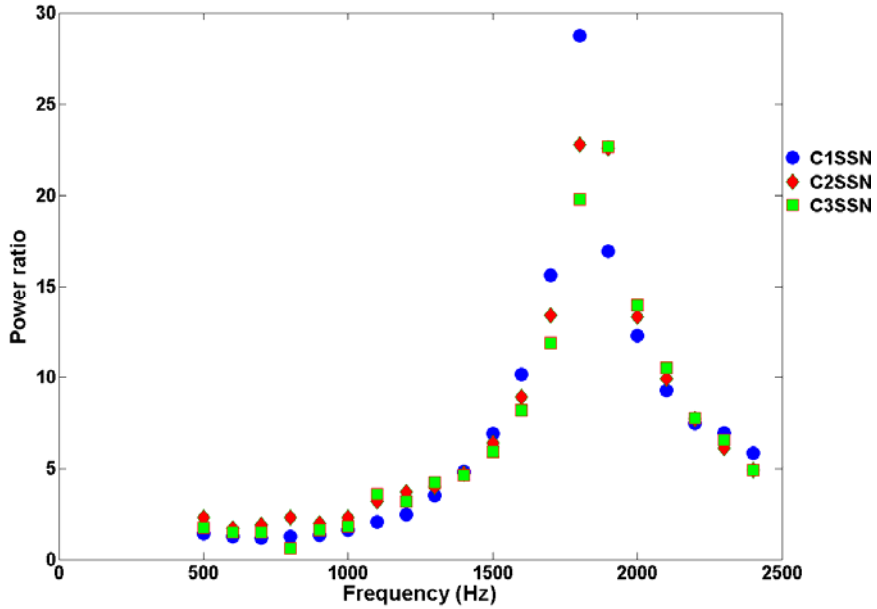

Figure 16. Attenuation of incident (1,0) mode wave, liner treatment on both sides, no flow, compares straight (C1SSN), ½ D offset (C2SSN), and 1D offset curved (C3SSN) liners

The trend of decreasing attenuation at the peak with increasing curvature is also seen in Figure 16 in which the incident wave is order (1,0).

When incident wave is horizontal order 1 mode the frequency of peak attenuation shifts up to 1900 Hz. This is shown in Figure 17 for (0,1) mode incident. As was observed for the 0 order horizontal modes incident, the peak attenuation decreases as the curvature increases. Moreover, the attenuation with the straight configuration is greater for all frequencies than it is for the curved configuration. This same trend is observed for the (1,1) and (2,1) modes incident, not shown here.

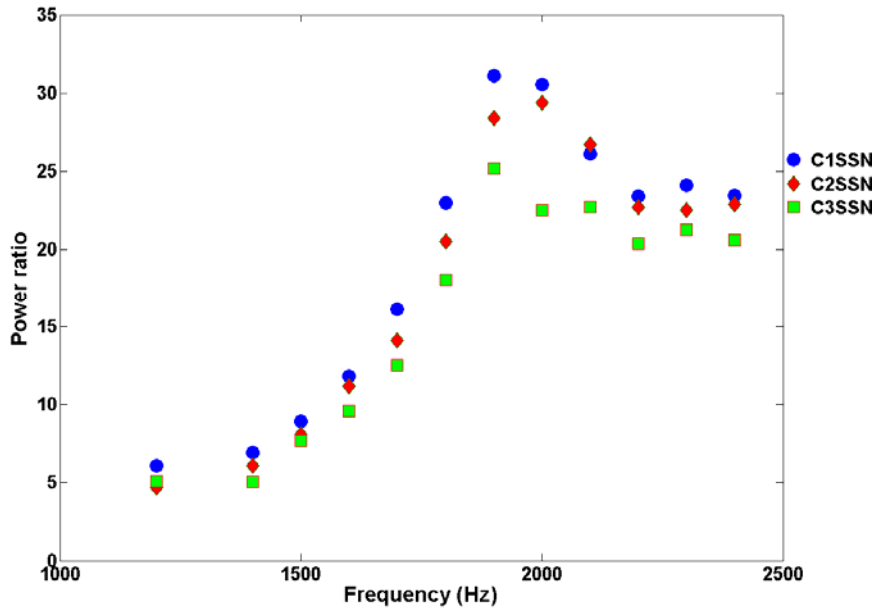

Figure 17. Attenuation of incident (0,1) mode wave, liner treatment on both walls, no flow, compares straight liner (C1SSN), ½ D offset curved (C2SSN), and 1D offset curved (C3SSN)

D. Comparison to CDUCT-LaRC

The attenuation of the liner is estimated using CDUCT-LaRC and the results are compared to the measured data. CDUCT-LaRC uses as input the modal amplitudes determined from measured data upstream of the liner test section. The impedance of the liner is also required by CDUCT-LaRC. The normal incidence impedance for the straight and curved liner panels was not measured but is calculated based on values measured in the Grazing Incidence Tube facility at NASA Langley for a liner sample of similar design. It is assumed that the liner impedance is the same whether the liner configuration is straight or curved. The rigid wall impedance was not measured but is assumed to be large: $\left(\frac{Z}{\rho c}\right)_{HW} = 10^{23} + i(10^{23})$.

Figure 18 compares measured attenuation to the attenuation predicted by CDUCT-LaRC for (0,0) mode wave incident on the liner test section with the 1D offset curved liner

panel on both sides (C3SSN). The curves compare favorably at frequencies below the peak attenuation. The frequency of peak attenuation, 1800 Hz, is the same for both measured and CDUCT-LaRC. CDUCT-LaRC overestimates the attenuation at frequencies above the peak. It is felt that the agreement between measured and analytic results is sufficient to warrant further comparisons.

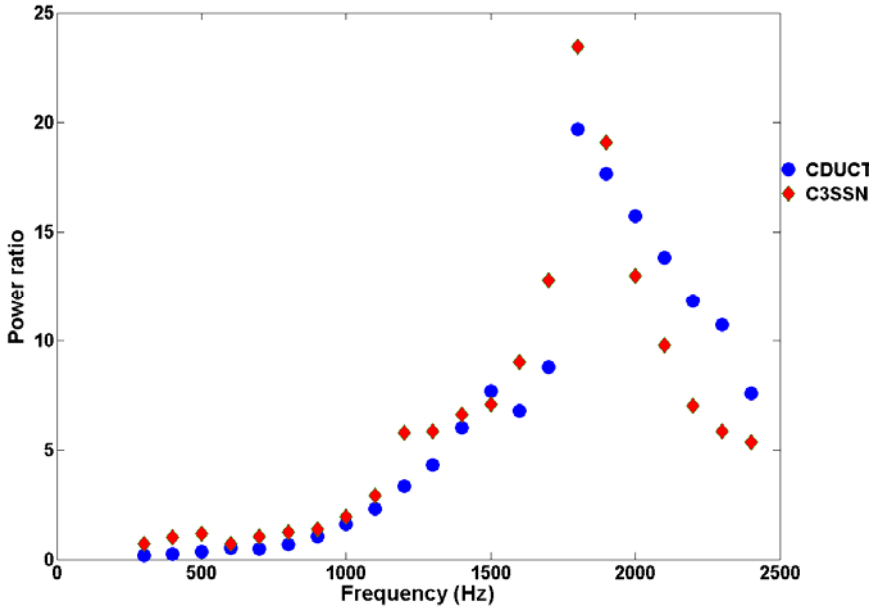

Figure 18. Comparison of predicted to measured attenuation, (0,0) mode incident on liner test section with 1 D offset curved liner, both sides (C3SSN), no flow.

Figure 19 compares measured to CDUCT-LaRC for the case in which the left wall of the curved duct is rigid and the right wall is treated, (C3HSN), for (0,0) mode incident. The comparison is reasonable both below and above the peak frequency. CDUCT-LaRC underestimates the attenuation at the peak. However, like the measured case, the peak attenuation is less than ½ the attenuation for the case in which both sides are treated. The reason this is so in the measured data was found to be due to scattering of the incident mode energy into the less attenuated (0,1) mode. This also found to be the case in the CDUCT-LaRC computation as is shown in Figure 20, the predicted modal distribution of the sound intensity downstream of the liner test section. The mode distribution compares quite favorably with the measured mode distribution for (0,0) mode incident on liner C3HSN, Figure 11.

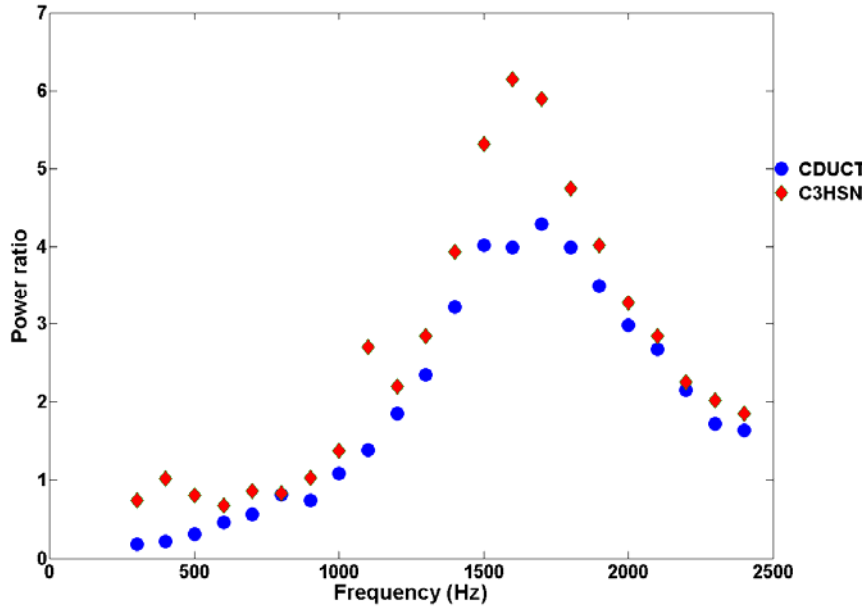

Figure 19. Comparison of predicted to measured attenuation, (0,0) mode incident on liner test section with 1 D offset curved liner, one side treated, one side rigid (C3HSN), no flow.

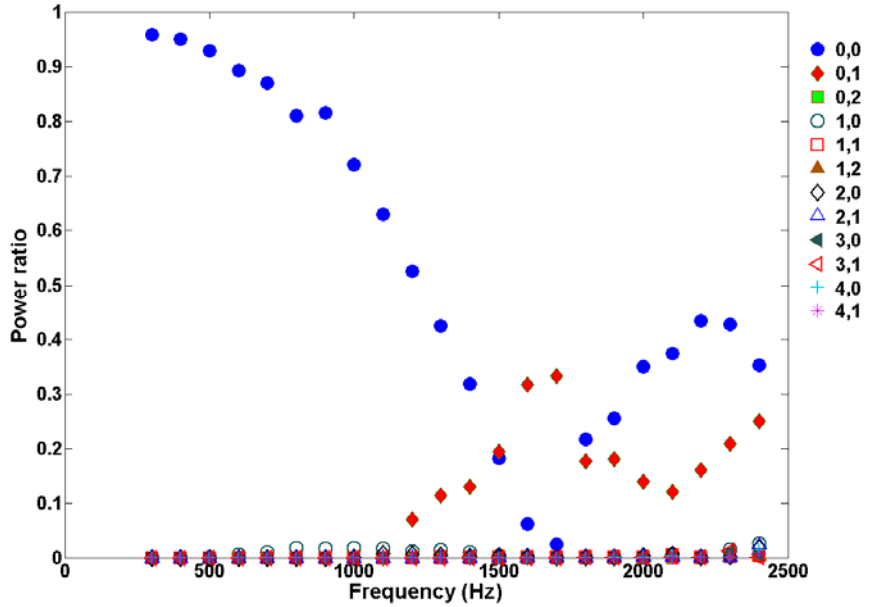

Figure 20. Modal energy distribution computed by CDUCT-LaRC downstream of liner test section with 1D offset curved test section lined on one side (C3HSN), (0,0) mode wave incident, no flow.

The configuration C3HHN, curved 1 D offset hard wall both sides, is evaluated by CDUCT-LaRC for the (0,0) mode incident. The average attenuation over the frequency range 500 to 2500 Hz is calculated at 0.39 dB so curvature accounts for less than 0.5 dB

attenuation. It is shown in Figure 21 that the incident mode energy transfers to the (0,1) mode, as was observed in the measured data, Figure 7. Unlike the measurement, the (0,0) mode does not start to decay until the (0,1) mode cuts on. This is reflective of the relatively more compliant wall surface of the fabricated hard wall in the CDTR experiment than is assumed in CDUCT-LaRC calculations. This difference in impedance accounts for the 1 dB greater attenuation in the measured data than is predicted by CDUCT-LaRC.

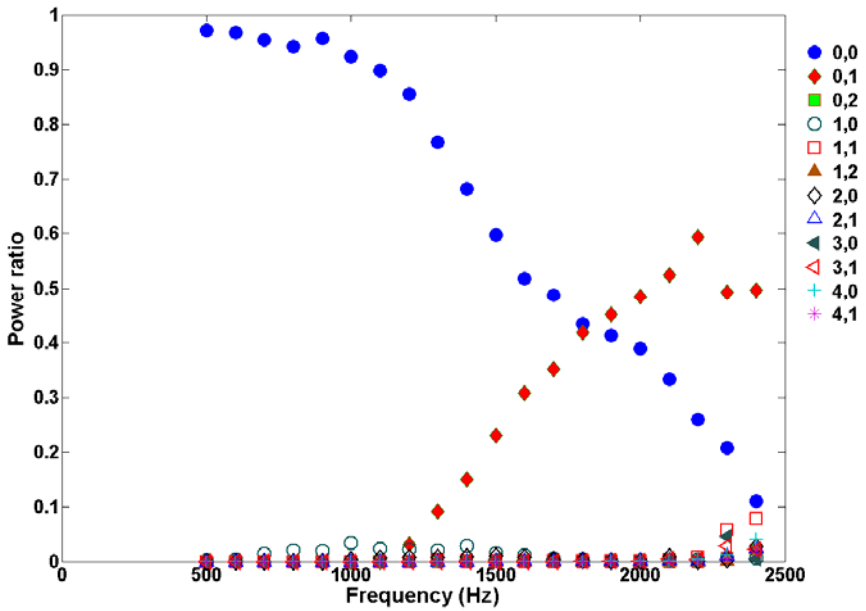

Figure 21. Modal energy distribution computed by CDUCT-LaRC downstream of liner test section with 1D offset curved test section hard wall (C3HHN), (0,0) mode wave incident, no flow.

V. Summary and Conclusions

The Curved Duct Test Rig has been used successfully to provide acoustic data for various liner test section samples both straight and curved including acoustically rigid sides, acoustically soft sides, and combinations. The control system provides user-specified incident sound level and mode designation at any frequency up to 2400 Hz. Liner samples of configuration applicable to an aircraft nacelle have been fabricated and evaluated. The curved samples include ½ duct width and 1 duct width offsets with constant rate of curvature. Rigid wall equivalents, in which the perforate face sheet is replaced by a solid face sheet, have also been fabricated and evaluated.

The curvature is felt to account for 0.5 dB attenuation for (0,0) mode wave incident. The hard wall curved path, however, redistributes the incident power. Modes of horizontal order 0 scatter into higher, horizontal order 1 modes. Modes of horizontal order 1 scatter into lower, horizontal order 0 modes. The data are not sufficient to assess the scattering of higher order horizontal modes.

When one wall of the liner test section is lined and the other wall is acoustically rigid, the peak attenuation of horizontal order 0 modes is 1600 Hz. There is little difference observed between the curved and straight flow paths. The peak attenuation shifts upward to 2000 Hz when horizontal order 1 modes are incident on the liner test section. Incident sound energy scatters into less attenuated modes, and scattering of incident sound significantly generally reduces the overall attenuation.

When both walls of the liner test section are acoustically lined, the peak attenuation of horizontal order 0 modes is considerably more than double the attenuation in the one wall lined configuration. This is because incident energy does not scatter into less attenuated modes. Curvature does not make a significant difference in the attenuation, except at the peak of the attenuation curve. The straight lined configuration provides the highest peak attenuation and peak attenuation decreases with increasing curvature. This is conjectured to be due either to the effect of angle of incidence of the sound relative to the liner surface or to the effective angle of the resonator cavities. This area is the subject of on-going research.

Comparison of the measured results to CDUCT-LaRC is quite favorable. The mode scattering that was observed in the measured data as a function of duct curvature is also seen in the computed results. As a consequence of mode scattering, the attenuation in the case of one wall treated and the other rigid is less than half of the attenuation when both walls are treated. The effect of this asymmetry seen in the CDUCT-LaRC results is the same as is observed in the measured results.

Acknowledgements

The authors are grateful for contributions made to the successful completion of the project by Christal Kellam of NASA LaRC. They also wish to acknowledge Goodrich Aerospace for fabrication of the duct liner samples used in these tests.

References

1. Tyler, J.M. and Sofrin, T.G., "Axial Flow Compressor Noise Studies", SAE Transactions, vol. 70, 1962, pp 309-332

2. Jones, M.G. and Parrott, T.L., “Evaluation of a multi-point method for determining acoustic impedance,” Journal of Mechanical Systems and Signal Processing, Vol. 3, No. 1, 1989, pp. 15-35.

3. Jones, M.G., Parrott, T.L., and Watson, W.R., “Comparison of Acoustic Impedance Eduction Techniques for Locally-Reacting Liners,” AIAA Paper 2003-3306, Proceedings of the 9th AIAA/CEAS Aeroacoustics Conference & Exhibit, May, 2003.

4. Minner, G.L. and Rice, E.J., "Computer method for design of acoustic liners for turbofan engines", NASA TM X-3317, 1976

5. Bielak, G, Gallman, J, Kunze, R., Murray, P, Premo, J,. Kosanchick, M., Hersh, A., Celano, J., Walker, B., Yu, J., Kwan, H., Chiou, S., Kelly, J., Betts, J., Follet, J., and Thomas, R., "Advanced Nacelle Acoustic Lining Concepts Development", NASA/CR-2002-211672, 2002

6. Jones, M. G., Tracy, M. B., Watson, W. R., and Parrott, T. L.," Effects of liner geometry on acoustic impedance", AIAA 2002-2446, 2002

7. Jones, M.G., Watson, W.R., Tracy, M.B., and Parrott, T.L., "Comparison of Two Waveguide Methods for Educing Liner Impedance in Grazing Flow," AIAA Journal, Vol. 42, No. 2, 2004, pp.232-240.

8. Cummings, A. "Sound transmission in curved duct bends", Journal of Sound and Vibration, volume 35, pp 451-477, 1974

9. Furnell, G. D. and Bies, D. A., "Characteristics of modal wave propagation within longitudinally curved acoustic waveguides", Journal of Sound and Vibration, volume 130, pp 405-423, 1989

10. Fuller, C.R. and Bies, D.A., "Propagation of sound in a curved bend containing a curved axial partition", Journal of the Acoustical Society of America, volume 63, pp 681-686, 1978

11. Boija, S. and Nilsson, B., "Reflection of sound at area expansions in a flow duct", Journal of Sound and Vibration, volume 260 pp. 477–498, 2003

12. A. McAlpine, A. and Wright, M.C.M., "Acoustic scattering by a spliced turbofan inlet duct liner at supersonic fan speeds", Journal of Sound and Vibration volume 292, pp 911–934, 2006

13. Gerhold, C.H., Cabell, R.H., and Brown, M.C., "Development of an Experimental Rig for Investigation of Higher Order Modes in Ducts", AIAA paper AIAA-2006-2637, 2006.

14. Gerhold, C.H., Brown, M. C., Watson, W. R. ,and. Jones, M. G ., "Investigation Of Liner Characteristics In The NASA Langley Curved Duct Test Rig", AIAA-2007-3532, 2007

15. Morfey, C.L., "Sound Transmission and Generation in Ducts with Flow", Journal of Sound and Vibration, volume 14, number 2, pp 37-55, 1971.

16. Nark, D. M., Farassat, F., Pope, D. S., and Vatsa, V., "The development of the ducted fan noise propagation and radiation code cduct-larc", AIAA Paper 2003-3242, 2003.

17. Dougherty, R. P., "A wave-splitting technique for nacelle acoustic propagation", AIAA Paper 97-1652, 1997.

18. Dougherty, R. P., "A parabolic approximation for flow effects on sound propagation in nonuniform, softwall, ducts", AIAA Paper 99-1822, 1999.

19. Parrott, T.L., Jones, M.G., and Homeijer, B., "Effect Of Resonator Axis Skew On Normal Incidence Impedance", AIAA paper 2003-3307, 2003.

20. Motsinger, R.E. and Kraft, R.E., "Design and Performance of Duct Acoustic Treatment", pp 165-206, NASA reference publication 1258, "Aeroacoustics of Flight Vehicles: Theory and Practice, volume 2: Noise Control", Hubbard, H.H., ed, 1991

Appendix A. Additional figures

The figures in this appendix are shown to illustrate trends in the mode distribution or overall attenuation of higher order modes that were observed in the experiments.

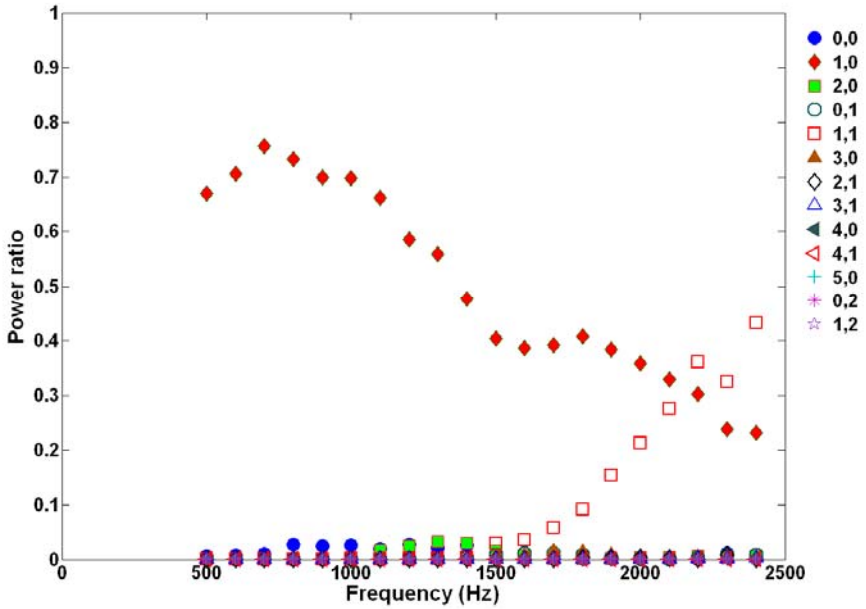

Figure A-1. Modal energy distribution downstream of liner test section with curved hard wall sample (C3HHN), (1,0) mode wave incident, no flow.

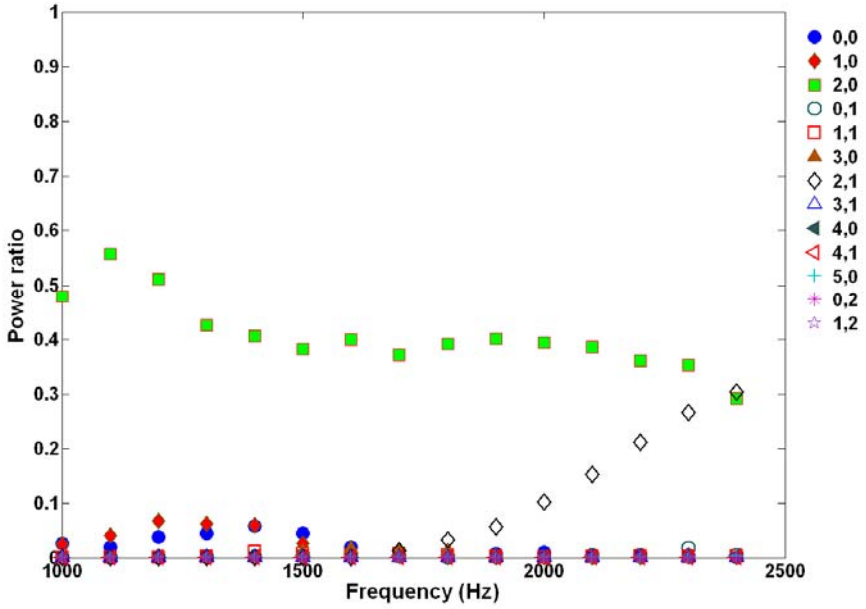

Figure A-2. Modal energy distribution downstream of liner test section with curved hard wall sample (C3HHN), (2,0) mode wave incident, no flow.

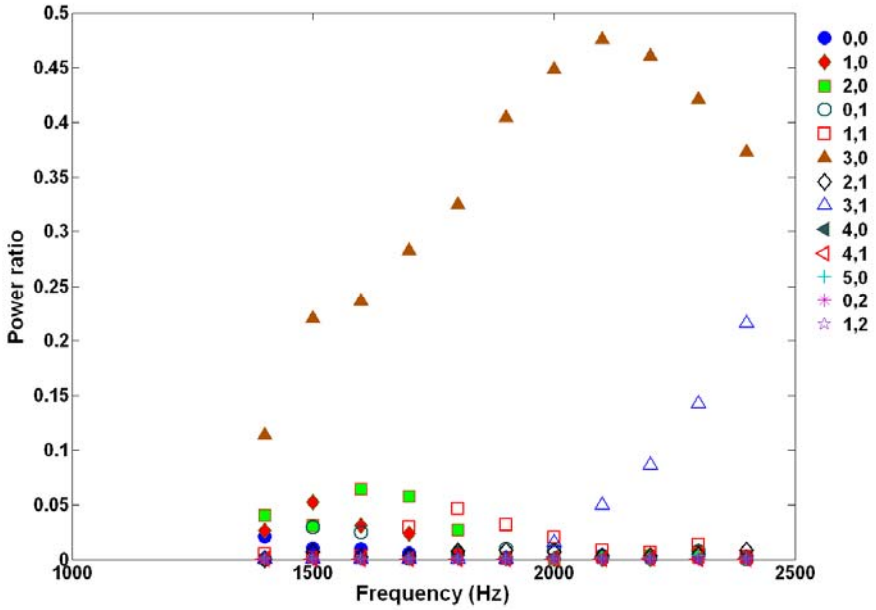

Figure A-3. Modal energy distribution downstream of liner test section with curved hard wall sample (C3HHN), (3,0) mode wave incident, no flow.

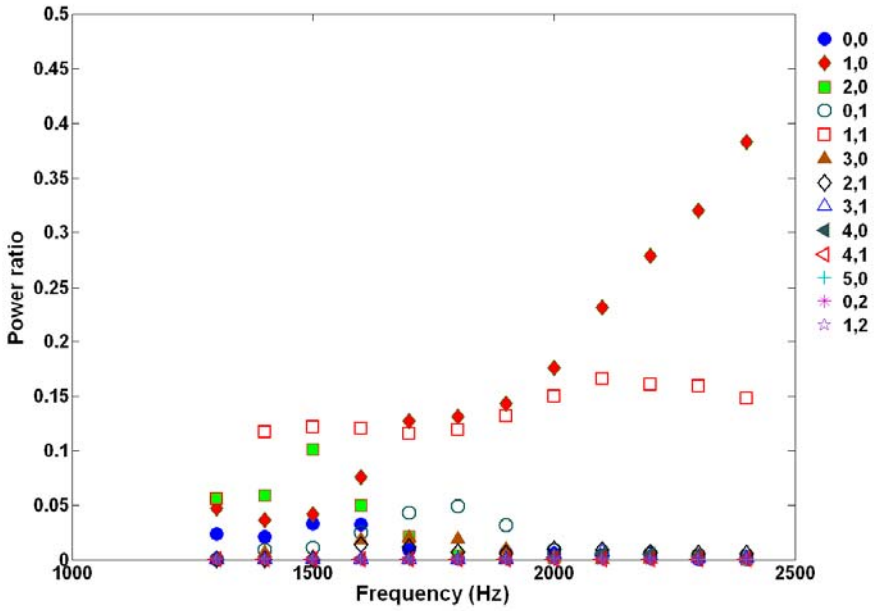

Figure A-4. Modal energy distribution downstream of liner test section with curved hard wall sample (C3HHN), (1,1) mode wave incident, no flow.

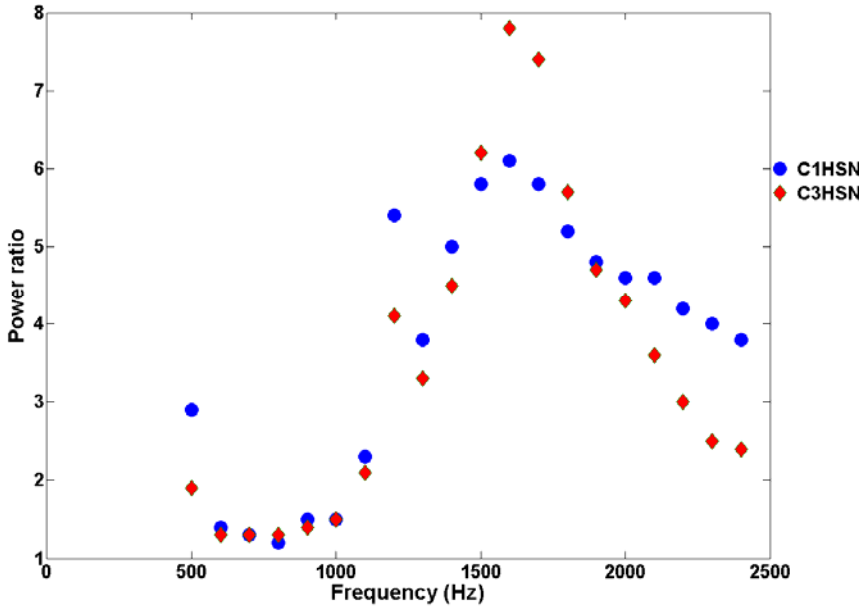

Figure A-5. Attenuation of (1,0) mode wave incident on liner test section with right side acoustically treated, left side hard wall. Compares straight liner sample (C1HSN) with 1D offset curved sample (C3HSN), no flow

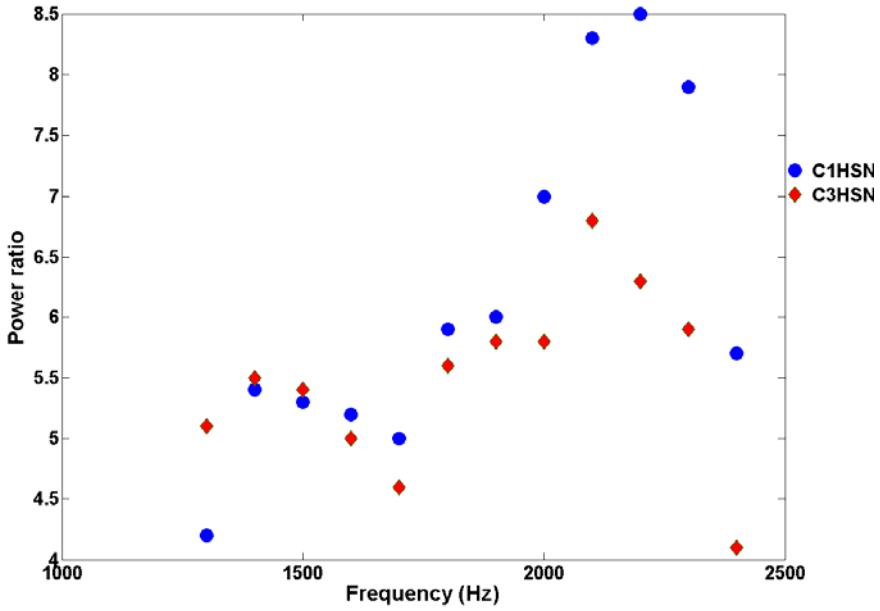

Figure A-6. Attenuation of (1,1) mode wave incident on liner test section with right side acoustically treated, left side hard wall. Compares straight liner sample (C1HSN) with 1D offset curved sample (C3HSN), no flow

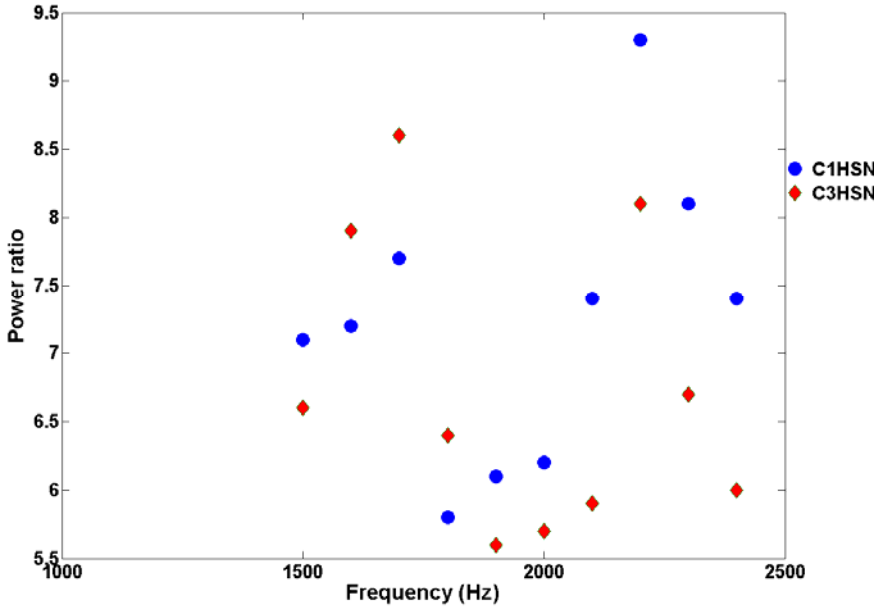

Figure A-7. Attenuation of (2,1) mode wave incident on liner test section with right side acoustically treated, left side hard wall. Compares straight liner sample (C1HSN) with 1D offset curved sample (C3HSN), no flow

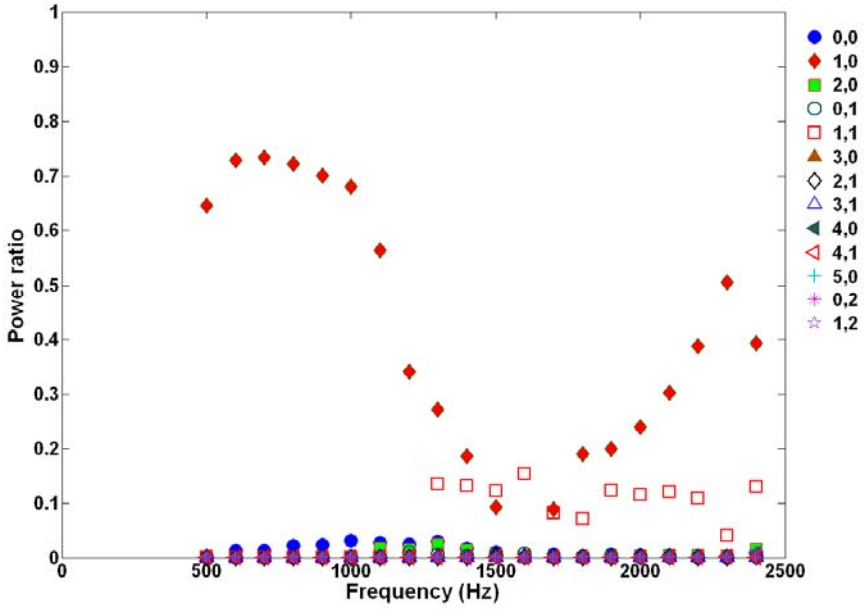

Figure A-8. Modal energy distribution downstream of liner test section with 1D offset curved test section lined on one side (C3HSN), (1,0) mode wave incident, no flow.